

## Searching for the odderon in exclusive $pp \rightarrow pp\phi$ and $pp \rightarrow pp\phi\phi$ reactions at the LHC

P. Lebedowicz,<sup>a,\*</sup> O. Nachtmann<sup>b</sup> and A. Szczurek<sup>a,†</sup>

<sup>a</sup>*Institute of Nuclear Physics Polish Academy of Sciences  
Radzikowskiego 152, PL-31342 Kraków, Poland*

<sup>b</sup>*Institut für Theoretische Physik, Universität Heidelberg  
Philosophenweg 16, D-69120 Heidelberg, Germany*

*E-mail: [Piotr.Lebedowicz@ifj.edu.pl](mailto:Piotr.Lebedowicz@ifj.edu.pl),*

*[O.Nachtmann@thphys.uni-heidelberg.de](mailto:O.Nachtmann@thphys.uni-heidelberg.de), [Antoni.Szczurek@ifj.edu.pl](mailto:Antoni.Szczurek@ifj.edu.pl)*

We discuss the  $pp \rightarrow pp\phi$  and  $pp \rightarrow pp\phi\phi$  reactions in identifying the odderon, the charge conjugation  $C = -1$  counterpart of the  $C = +1$  pomeron. Recently proposed tensor-pomeron and vector-odderon model for soft high-energy reactions is applied. For the  $pp \rightarrow pp\phi$  reaction the photon-pomeron fusion is the dominant process and the odderon-pomeron fusion is an interesting alternative. Adding odderon exchange improves description of the proton-proton angular correlations and the  $dP_t$  dependence measured by the WA102 collaboration. The  $pp \rightarrow pp\phi\phi$  process via pomeron-pomeron fusion is advantageous one as here the odderon does not couple to protons. The observation of large  $\phi\phi$  invariant masses and large rapidity distance between  $\phi$  mesons seems well suited to distinguish the odderon contribution from other contributions. Comparisons with exclusive data for single and double  $\phi$  production from the WA102 experiment are made and predictions for LHC experiments are presented.

\*\*\* *The European Physical Society Conference on High Energy Physics (EPS-HEP2021)*, \*\*\*

\*\*\* *26-30 July 2021* \*\*\*

\*\*\* *Online conference, jointly organized by Universität Hamburg and the research center DESY* \*\*\*

---

\*Speaker

†Also at *College of Natural Sciences, Institute of Physics, University of Rzeszów, Pigońia 1, PL-35310 Rzeszów, Poland.*

## 1. Introduction

The odderon was introduced on the basis of asymptotic theorems [1]. It was predicted in QCD as a colourless charge-conjugation  $C$ -odd three-gluon bound state exchange [2, 3]. Therefore, the search for the odderon is crucial in order to confirm the validity of QCD. A recent analysis by the D0 and TOTEM Collaborations [4] provides experimental evidence that the odderon is needed to describe elastic scattering at high energies [5]. It is of great importance to study possible odderon effects in other reactions. As was discussed in [6] exclusive diffractive  $\phi(1020)$  and  $J/\psi$  production by the pomeron-odderon fusion in high-energy  $pp$  and  $p\bar{p}$  collisions is a direct probe for a possible odderon exchange. We shall argue here that the central exclusive production (CEP) of a  $\phi\phi$  state offers a very nice way to look for odderon effects as suggested in [7].

In this contribution we will be concerned with CEP of single  $\phi$  observed in the  $K^+K^-$  or  $\mu^+\mu^-$  channels and of double  $\phi$  in the  $K^+K^-K^+K^-$  final state as a possible source of information for odderon exchange in  $pp$  collisions. The presentation is based on [8, 9] where all details and many more results can be found. At high energies the  $pp \rightarrow pp\phi$  reaction should be mainly due to photon-pomeron fusion mechanism and the odderon-pomeron fusion mechanism (Fig. 1 (a)) is an interesting addition. The  $pp \rightarrow pp\phi\phi$  reaction should be mainly due to double-pomeron exchange with resonant production at low  $\phi\phi$  invariant masses and the continuum processes at higher  $M_{\phi\phi}$ . The process with an intermediate  $\hat{t}/\hat{u}$ -channel odderon exchange (Fig. 1 (b)) seems to be a good candidate for the odderon searches, as it does not involve the coupling of the odderon to the proton.

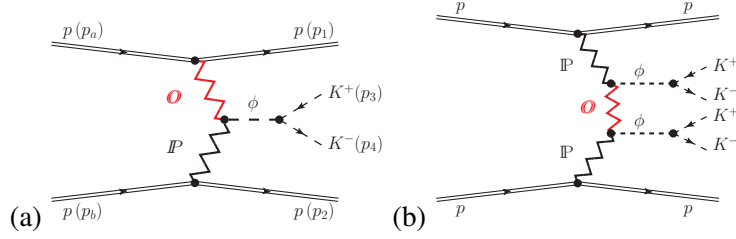


**Figure 1:** Diagrams for (a) single  $\phi$  production via odderon-pomeron fusion, and (b) double  $\phi$  production via odderon exchange. There is also diagram with the protons interchanged,  $(p(p_a), p(p_1)) \leftrightarrow (p(p_b), p(p_2))$ .

We treat our reactions in the tensor-pomeron and vector-odderon approach as introduced in [10]. This approach has a good basis from nonperturbative QCD using functional integral techniques [11]. We describe the pomeron and the  $C = +1$  reggeons as effective rank 2 symmetric tensor exchanges, the odderon and  $C = -1$  reggeons as effective vector exchanges. There are by now many successful applications of the tensor-pomeron model to two-body hadronic reactions [12], to DIS structure functions at low  $x$ , to photoproduction, and especially to CEP reactions:  $p + p \rightarrow p + X + p$ , where  $X = \eta, \eta', f_0, f_1, f_2, \pi^+\pi^-, p\bar{p}, K\bar{K}, 4\pi, 4K, \rho^0, \phi, \phi\phi, K^{*0}\bar{K}^{*0}$ ; see e.g. [8, 9, 13–16].

## 2. Formalism

As an example, we consider the single CEP of  $\phi(1020)$  meson

$$p(p_a, \lambda_a) + p(p_b, \lambda_b) \rightarrow p(p_1, \lambda_1) + p(p_2, \lambda_2) + [\phi(p_{34}) \rightarrow \mu^+(p_3, \lambda_3) + \mu^-(p_4, \lambda_4)]. \quad (1)$$

Here  $p_{a,b}, p_{1,2}$  and  $\lambda_{a,b}, \lambda_{1,2} = \pm\frac{1}{2}$  denote the four-momenta and helicities of the protons, and  $p_{3,4}$  and  $\lambda_{3,4} = \pm\frac{1}{2}$  denote the four-momenta and helicities of the muons, respectively. The Born-level

amplitude for the diffractive production of the  $\phi$  via odderon-pomeron fusion can be written as

$$\begin{aligned} \mathcal{M}^{(\mathbb{O}\mathbb{P})} = & (-i)\bar{u}(p_1, \lambda_1) i\Gamma_{\mu}^{(\mathbb{O}pp)}(p_1, p_a) u(p_a, \lambda_a) i\Delta^{(\mathbb{O})\mu\rho_1}(s_1, t_1) i\Gamma_{\rho_1\rho_2\alpha\beta}^{(\mathbb{P}\mathbb{O}\phi)}(-q_1, p_{34}) i\Delta^{(\phi)\rho_2\kappa}(p_{34}) \\ & \times \bar{u}(p_4, \lambda_4) i\Gamma_{\kappa}^{(\phi\mu\mu)}(p_3, p_4) v(p_3, \lambda_3) i\Delta^{(\mathbb{P})\alpha\beta,\delta\eta}(s_2, t_2) \bar{u}(p_2, \lambda_2) i\Gamma_{\delta\eta}^{(\mathbb{P}pp)}(p_2, p_b) u(p_b, \lambda_b). \end{aligned} \quad (2)$$

The kinematic variables are  $p_{34} = p_3 + p_4$ ,  $q_1 = p_a - p_1$ ,  $q_2 = p_b - p_2$ ,  $t_1 = q_1^2$ ,  $t_2 = q_2^2$ ,  $s = (p_a + p_b)^2$ ,  $s_1 = (p_1 + p_{34})^2$ ,  $s_2 = (p_2 + p_{34})^2$ . The full amplitude  $\mathcal{M}^{(\mathbb{O}\mathbb{P})} + \mathcal{M}^{(\mathbb{P}\mathbb{O})}$  includes the  $pp$ -rescattering corrections calculated in the one-channel eikonal approximation.

The effective pomeron propagator and the pomeron-proton vertex function are as follows [10]:

$$i\Delta_{\mu\nu,\kappa\lambda}^{(\mathbb{P})}(s, t) = \frac{1}{4s} \left( g_{\mu\kappa}g_{\nu\lambda} + g_{\mu\lambda}g_{\nu\kappa} - \frac{1}{2}g_{\mu\nu}g_{\kappa\lambda} \right) (-is\alpha'_{\mathbb{P}})^{\alpha_{\mathbb{P}}(t)-1}, \quad (3)$$

$$i\Gamma_{\mu\nu}^{(\mathbb{P}pp)}(p', p) = -i3\beta_{\mathbb{P}NN} F_1((p' - p)^2) \left\{ \frac{1}{2} [\gamma_{\mu}(p' + p)_{\nu} + \gamma_{\nu}(p' + p)_{\mu}] - \frac{1}{4}g_{\mu\nu}(\not{p}' + \not{p}) \right\}, \quad (4)$$

where  $\beta_{\mathbb{P}NN} = 1.87 \text{ GeV}^{-1}$  and  $t = (p' - p)^2$ . For simplicity we use the electromagnetic Dirac form factor  $F_1(t)$  of the proton. The pomeron trajectory  $\alpha_{\mathbb{P}}(t)$  is assumed to be of standard linear form:  $\alpha_{\mathbb{P}}(t) = \alpha_{\mathbb{P}}(0) + \alpha'_{\mathbb{P}} t$ , with  $\alpha_{\mathbb{P}}(0) = 1.0808$  and  $\alpha'_{\mathbb{P}} = 0.25 \text{ GeV}^{-2}$ .

Our ansatz for the  $C = -1$  odderon follows (3.16), (3.17) and (3.68), (3.69) of [10]:

$$i\Delta_{\mu\nu}^{(\mathbb{O})}(s, t) = -ig_{\mu\nu} \frac{\eta_{\mathbb{O}}}{M_0^2} (-is\alpha'_{\mathbb{O}})^{\alpha_{\mathbb{O}}(t)-1}, \quad (5)$$

$$i\Gamma_{\mu}^{(\mathbb{O}pp)}(p', p) = -i3\beta_{\mathbb{O}pp} M_0 F_1((p' - p)^2) \gamma_{\mu}, \quad (6)$$

where  $\eta_{\mathbb{O}}$  is a parameter with value  $\eta_{\mathbb{O}} = \pm 1$ ;  $M_0 = 1 \text{ GeV}$  is inserted for dimensional reasons. We assumed  $\beta_{\mathbb{O}pp} = 0.1 \times \beta_{\mathbb{P}NN}$ . We take  $\alpha_{\mathbb{O}}(t) = \alpha_{\mathbb{O}}(0) + \alpha'_{\mathbb{O}} t$ . In our calculations we shall choose as default values  $\alpha_{\mathbb{O}}(0) = 1.05$ ,  $\alpha'_{\mathbb{O}} = 0.25 \text{ GeV}^{-2}$ , and  $\eta_{\mathbb{O}} = -1$ ; see [8].

For the  $\mathbb{P}\mathbb{O}\phi$  vertex we use an ansatz analogous to the  $\mathbb{P}\phi\phi$  vertex (see (3.48)–(3.50) of [9])

$$\begin{aligned} i\Gamma_{\rho_1\rho_2\alpha\beta}^{(\mathbb{P}\mathbb{O}\phi)}(-q_1, p_{34}) = & i \left[ 2a_{\mathbb{P}\mathbb{O}\phi} \Gamma_{\rho_2\rho_1\alpha\beta}^{(0)}(p_{34}, -q_1) - b_{\mathbb{P}\mathbb{O}\phi} \Gamma_{\rho_2\rho_1\alpha\beta}^{(2)}(p_{34}, -q_1) \right] \\ & \times F_M(q_2^2) F_M(q_1^2) F^{(\phi)}(p_{34}^2). \end{aligned} \quad (7)$$

Here we use the relations (3.20) of [10] and as in (3.49) of [9] we take the factorised form for the  $\mathbb{P}\mathbb{O}\phi$  form factor; see [8]. The coupling parameters  $a_{\mathbb{P}\mathbb{O}\phi}$ ,  $b_{\mathbb{P}\mathbb{O}\phi}$  in (7) and the cut-off parameter  $\Lambda_{0,\mathbb{P}\mathbb{O}\phi}^2$  in  $F_M(t) = 1/(1 - t/\Lambda_{0,\mathbb{P}\mathbb{O}\phi}^2)$  could be adjusted to experimental data. The WA102 data allow us to determine the respective coupling constants as  $a_{\mathbb{P}\mathbb{O}\phi} = -0.8 \text{ GeV}^{-3}$ ,  $b_{\mathbb{P}\mathbb{O}\phi} = 1.6 \text{ GeV}^{-1}$ , and  $\Lambda_{0,\mathbb{P}\mathbb{O}\phi}^2 = 0.5 \text{ GeV}^2$  from [8]. We describe the transition  $\phi \rightarrow \gamma^* \rightarrow \mu^+\mu^-$ , by  $i\Gamma_{\kappa}^{(\phi\mu\mu)}(p_3, p_4) = ig_{\phi\mu^+\mu^-} \gamma_{\kappa}$  with  $g_{\phi\mu^+\mu^-} = (6.92 \pm 0.08) \times 10^{-3}$  [8].

For high energies and central  $\phi$  production we expect the reaction (1) to be dominated by the fusion processes  $\gamma\mathbb{P} \rightarrow \phi$  and  $\mathbb{O}\mathbb{P} \rightarrow \phi$ . The parameters in the first process ( $\phi$  photoproduction) were fixed to describe the HERA data taking into account the  $\phi$ - $\omega$  mixing effect. For the odderon-exchange process we used the ansätze from [10] and tried to get information on the odderon parameters and couplings from the comparison to the WA102 data for the  $pp \rightarrow pp\phi$  and  $pp \rightarrow pp\phi\phi$  reactions. Of course, at the relatively low c.m. energy of the WA102 experiment,  $\sqrt{s} = 29.1 \text{ GeV}$ , we have to include also subleading contributions with reggeized-vector-meson (or reggeon) exchanges; see [8, 9].

### 3. Results

As was presented in [8] inclusion of the odderon-exchange contribution significantly improves the description of the  $pp$  azimuthal correlations ( $\phi_{pp}$  is angle between the transverse momentum vectors  $\mathbf{p}_{t,1}$ ,  $\mathbf{p}_{t,2}$  of the outgoing protons) and the  $dP_t = |\mathbf{p}_{t,2} - \mathbf{p}_{t,1}|$  dependence of  $\phi$  CEP measured by the WA102 collaboration [17]. In the left panel of figure 2 we present the  $\mathbb{O}$ - $\mathbb{P}$  contribution (approach II of [8]) together with the  $\gamma$ - $\mathbb{P}$  contribution and with the subleading terms. Adding odderon exchange term improves description of the WA102 data. Having fixed the parameters of model to the WA102 data we show our predictions for the LHC at  $\sqrt{s} = 13$  TeV. The absorption effects were included in the calculations. We considered different dedicated observables.

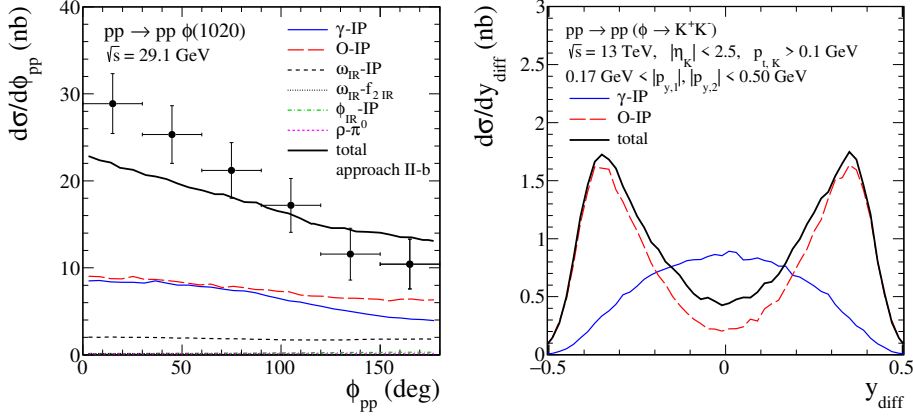


**Figure 2:** Left panel: The distributions in  $\phi_{pp}$  together with the WA102 experimental data points for  $\sqrt{s} = 29.1$  GeV normalized to the central value of the total cross section  $\sigma_{\text{exp}} = 60$  nb from [17]. The coherent sum of all considered terms is shown by the black solid line. Right panel: The distribution in rapidity difference between kaons for the reaction  $pp \rightarrow pp(\phi \rightarrow K^+K^-)$  for the ATLAS-ALFA kinematics.

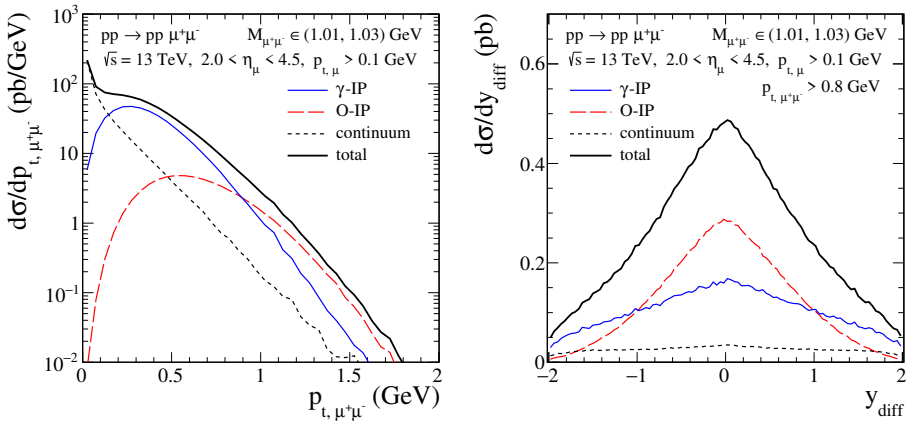


**Figure 3:** The distributions in transverse momentum of the  $\mu^+\mu^-$  pair (left) and in rapidity difference between muons (right) for the exclusive  $pp \rightarrow pp\mu^+\mu^-$  reaction for  $\sqrt{s} = 13$  TeV and  $M_{\mu^+\mu^-} \in (1.01, 1.03)$  GeV. The results for the  $\gamma$ - $\mathbb{P}$  and  $\mathbb{O}$ - $\mathbb{P}$  fusion terms, the  $\gamma\gamma \rightarrow \mu^+\mu^-$  continuum, and their coherent sum are presented.

In the right panel of figure 2 we show the distribution in  $y_{\text{diff}}$  (rapidity difference between kaons) for the  $pp \rightarrow pp(\phi \rightarrow K^+K^-)$  reaction. For the ATLAS-ALFA kinematics the absorption effects lead to a large damping of the cross sections for both the  $\gamma\text{-}\mathbb{P}$  and  $\mathbb{O}\text{-}\mathbb{P}$  mechanisms; see Table II of [8]. The  $y_{\text{diff}}$  and the angular distributions of kaons in the Collins-Soper frame seem particularly interesting for the  $K^+K^-$  final state. These angular distributions give information on the polarisation state of the produced  $\phi$  meson. According to our model, the polarisation of the  $\phi$  and, as a consequence, the angular distribution of the kaons in the Collins-Soper frame are very different for the  $\gamma\text{-}\mathbb{P}$ - and  $\mathbb{O}\text{-}\mathbb{P}$ -fusion processes. This should be a big asset for the odderon search.

Now we discuss the  $pp \rightarrow pp\mu^+\mu^-$  reaction (1) at forward rapidities and without measurement of protons relevant for LHCb. Here we focus on the limited invariant mass region around the  $\phi(1020)$  resonance. Figure 3 shows the distribution in transverse momentum of the  $\mu^+\mu^-$  pair. We can see that the low- $p_{t,\mu^+\mu^-}$  cut can be helpful to reduce the continuum and  $\gamma\text{-}\mathbb{P}$ -fusion terms. In the right panel we show the  $y_{\text{diff}}$  distribution when imposing in addition a cut  $p_{t,\mu^+\mu^-} > 0.8$  GeV. At  $y_{\text{diff}} = 0$  the  $\mathbb{O}\text{-}\mathbb{P}$  term should win with the  $\gamma\text{-}\mathbb{P}$  term. There is for both contributions a maximum at  $y_{\text{diff}} = 0$ . In this case the absolute normalization of the cross section or detailed studies of shape of distributions should provide a hint whether one observes the odderon effect.

Now we go to the double CEP of  $\phi$ . Figure 4 (left panel) shows the results including the  $f_2(2340)$  term and the continuum processes due to reggeized- $\phi$  and odderon exchanges. For the details how to calculate these processes see [9]. Inclusion of the odderon exchange improves the description of the WA102 data [18] for the  $pp \rightarrow pp\phi\phi$  reaction at higher  $M_{\phi\phi}$ . Here we show results for the odderon-exchange contribution with the parameters of our model fixed to the WA102 data [17] on single CEP of  $\phi$ ; see section IV A of [8]. In the right panel we show the distribution in four-kaon invariant mass for the LHCb experimental conditions. The small intercept of the  $\phi$ -reggeon exchange ( $\alpha_\phi(0) = 0.1$ ) makes the  $\phi$ -exchange contribution steeply falling with increasing  $M_{4K}$ . Therefore, the odderon exchange with an intercept  $\alpha_{\mathbb{O}}(0) \approx 1.0$  should be clearly visible in the region of large  $M_{4K}$  and also for large  $y_{\text{diff}}$  between the  $\phi$  mesons.

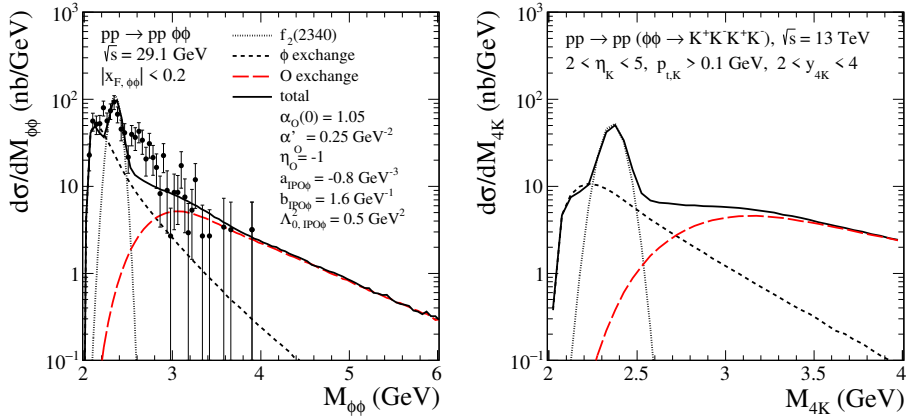


**Figure 4:** The distributions in  $\phi\phi$  invariant mass (left) for  $\sqrt{s} = 29.1$  GeV together with the WA102 data from [18] and (right) in  $M_{4K}$  for the LHCb kinematics. The short-dashed line corresponds to the reggeized- $\phi$ -exchange contribution, the dotted line corresponds to the  $f_2(2340)$  contribution, the red long-dashed line represents the  $\mathbb{O}$ -exchange contribution. The coherent sum of all terms is shown by the black solid line.

#### 4. Conclusions

- We have discussed in detail the  $pp \rightarrow pp\phi$  and  $pp \rightarrow pp\phi\phi$  reactions. For single  $\phi$  CEP at the LHC there are two basic processes: the relatively well known  $\gamma$ - $\mathbb{P}$  fusion and the rather elusive  $\mathbb{O}$ - $\mathbb{P}$  fusion. We fixed the parameters of the pomeron-odderon contribution to obtain a good description of the WA102 data [17, 18].
- We have estimated the integrated cross sections and several differential distributions at the LHC; see Table II of [8]. The main result of our analysis for  $pp \rightarrow pp(\phi \rightarrow K^+K^-)$  is that, the  $y_{\text{diff}}$  distributions are very different for the  $\gamma$ - $\mathbb{P}$ - and  $\mathbb{O}$ - $\mathbb{P}$ -fusion processes. The  $\mu^+\mu^-$  channel seems to be less promising in identifying the odderon exchange at least when only the  $p_{t,\mu}$  cuts are imposed. To observe a sizeable deviation from photoproduction a  $p_{t,\mu^+\mu^-} > 0.8$  GeV cut on the transverse momentum of the  $\mu^+\mu^-$  pair seems necessary. A combined analysis of both the  $K^+K^-$  and the  $\mu^+\mu^-$  channels should be the ultimate goal in searches for odderon.
- The  $pp \rightarrow pp\phi\phi$  process via odderon exchange [figure 1(b)] seems promising as here the odderon does not couple to protons. We find from our model that the odderon-exchange contribution should be distinguishable from other contributions for relatively large four-kaon invariant masses (outside of the region of resonances) and for large rapidity distance between the  $\phi$  mesons. Hence, to study this type of mechanism one should investigate “three-gap events” ( $p$ -gap- $\phi$ -gap- $\phi$ -gap- $p$ ). Experimentally, this should be a clear signature. We are looking forward to first experimental results on single and double  $\phi$  CEP at the LHC.

#### References

- [1] L. Łukaszuk and B. Nicolescu, *Lett. Nuovo Cim.* **8** (1973) 405.
- [2] J. Kwieciński and M. Praszalowicz, *Phys. Lett. B* **94** (1980) 413.
- [3] J. Bartels, *Nucl. Phys. B* **175** (1980) 365.
- [4] V. M. Abazov *et al.*, (TOTEM and D0 Collaborations), *Phys. Rev. Lett.* **127** (2021) 062003..
- [5] E. Martynov and B. Nicolescu, *Eur. Phys. J. C* **79** (2019) 461.
- [6] A. Schäfer, L. Mankiewicz, and O. Nachtmann, *Phys. Lett. B* **272** (1991) 419.
- [7] C. Ewerz, [arXiv:hep-ph/0306137](https://arxiv.org/abs/hep-ph/0306137) [hep-ph].
- [8] P. Lebedowicz, O. Nachtmann, and A. Szczurek, *Phys. Rev. D* **101** (2020) 094012.
- [9] P. Lebedowicz, O. Nachtmann, and A. Szczurek, *Phys. Rev. D* **99** (2019) 094034.
- [10] C. Ewerz, M. Maniatis, and O. Nachtmann, *Annals Phys.* **342** (2014) 31.
- [11] O. Nachtmann, *Annals Phys.* **209** (1991) 436.
- [12] C. Ewerz, P. Lebedowicz, O. Nachtmann, and A. Szczurek, *Phys. Lett. B* **763** (2016) 382.
- [13] P. Lebedowicz, O. Nachtmann, and A. Szczurek, *Annals Phys.* **344** (2014) 301.
- [14] P. Lebedowicz, O. Nachtmann, and A. Szczurek, *Phys. Rev. D* **93** (2016) 054015.
- [15] P. Lebedowicz, J. Leutgeb, O. Nachtmann, A. Rebhan, and A. Szczurek, *Phys. Rev. D* **102** (2020) 114003.
- [16] P. Lebedowicz, *Phys. Rev. D* **103** (2021) 054039.
- [17] A. Kirk, *Phys. Lett. B* **489** (2000) 29.
- [18] D. Barberis *et al.*, (WA102 Collaboration), *Phys. Lett. B* **432** (1998) 436.